Effect of structural parameters on fragility curves of highway bridges based on numerical simulation

by

Kazi R. Karim[1] and Fumio Yamazaki[2]

SUMMARY

To predict the extent of probable damages, fragility curves are found to be useful tools. It shows the probability of highway structure damages as a function of strong motion parameters. They allow estimating a level of damage probability for a known ground motion index. In this study, an analytical approach was adopted to develop the fragility curves for highway bridges based on numerical simulation. Four typical RC bridge piers and two RC bridge structures were considered of which one is a non-isolated system and the other one is an isolated system, and they were designed according to the seismic design code in Japan. A total of two hundred and fifty (250) strong motion records were selected from Japan, Taiwan and the United States. Using the selected acceleration records, nonlinear time history analyses were performed, and the damage indices for the bridge structures were obtained. Using the damage indices and ground motion parameters, fragility curves for the four bridge piers and the two bridge structures were constructed assuming a lognormal distribution. It is found that there is a significant effect on the fragility curves due to the variation of structural parameters. The relationship between the fragility curve parameters and over-strength ratio of the structures was also obtained performing a linear regression analysis. It is observed that fragility curve parameters show a strong correlation with the over-strength ratio of the structures. Based on the observed correlation between the fragility curve parameters and over-strength ratio of the structures, a simplified procedure was developed to construct the fragility curves using thirty (30) non-isolated bridge structures. The simplified method may be a very useful tool to construct the fragility curves for non-isolated highway bridge systems in Japan.

KEY WORDS: strong motion records; ground motion indices; highway bridges; damage analysis; regression model; fragility curves

INTRODUCTION

The actual damages [1, 2] to highway systems from recent earthquakes have emphasized the need for risk assessment of the existing highway transportation systems. The vulnerability assessment of bridges is useful for seismic retrofitting decisions, disaster response planning, estimation of direct monetary loss, and evaluation of loss of functionality of highway systems. Hence, it is important to know the degree of damages [1, 3, 4] of the highway bridge structures due to earthquakes. To estimate a damage level (slight, moderate, extensive, and complete) of highway bridge structures, fragility curves [1-3, 5] are found to be useful tool. Fragility curves show the relationship between the probability of highway structure damages and the ground motion indices. They allow estimating a damage level for a known ground motion index.

---

[1] Graduate Student, Institute of Industrial Science, the University of Tokyo, Japan.
[2] Professor, School of Advanced Technologies, Asian Institute of Technology, Thailand.

The 1995 Kobe earthquake, which is considered as one of the most damaging earthquakes in Japan, caused severe damages to expressway structures in Kobe area. Based on the actual damage data from the earthquake, a set of empirical fragility curves [1] was constructed. The empirical fragility curves give a general idea about the relationship between the damage levels of the highway structures and the ground motion indices. These fragility curves may be used for damage estimation of highway bridge structures in Japan. However, the empirical fragility curves do not specify the type of structure, structural performance (static and dynamic) and variation of input ground motion, and may not be applicable for estimating the level of damage probability for specific bridge structures [5]. It is assumed that structural parameters and input motion characteristics (e.g., frequency contents, phase, and duration) have influence to the damage of the structure for which there will be an effect on the fragility curves. Karim and Yamazaki [6] developed a set of analytical fragility curves for highway bridge piers considering the variation of input ground motions based on numerical simulation, and it was found that there is a significant effect of earthquake ground motions on fragility curves.

The objective of this study is to develop analytical fragility curves for highway bridges considering the variation of structural parameters based on numerical simulation. Four typical RC bridge piers [7] and two RC bridge structures are considered of which one is a non-isolated system and the other one is an isolated system, and they are designed [8, 9] according to the seismic design code [10] in Japan. A total of two hundred and fifty (250) strong motion records were selected from Japan, Taiwan and the United States as the input motions. Using the selected input motions, damage analyses of the bridge structures are performed, and the fragility curves are obtained assuming a lognormal distribution [1, 11]. A simplified procedure is also developed to construct the fragility curves using thirty (30) non-isolated bridge structures. The simplified method may be a very useful tool to construct the fragility curves for non-isolated highway bridge systems in Japan.

DEVELOPMENT OF FRAGILITY CURVES

Empirical fragility curves

Yamazaki *et al.* [1] developed a set of empirical fragility curves based on the actual damage data from the 1995 Kobe earthquake, and showed the relationship between the damages occurred to the expressway bridge structures and the ground motion indices. We do restrict to only a brief explanation regarding the empirical approach while details can be found elsewhere [1]. In this approach, the damage data of the JH expressway structures due to the Kobe earthquake were collected, and the ground motion indices along the expressways were estimated based on the estimated strong motion distribution using Kriging technique. The damage data and ground motion indices were related to each damage rank [1, 3, 4], and the damage ratio for each damage rank was obtained. Finally, using the damage ratio for each damage rank, the empirical fragility curves for the expressway bridge structures were constructed assuming a lognormal distribution.

Analytical fragility curves

Karim and Yamazaki [6] developed a set of analytical fragility curves for highway bridge piers based on numerical simulation and considering the variation of input ground motions. The procedures adopted for constructing the analytical fragility curves are briefly described below while details can be found elsewhere [6]. The steps for constructing the analytical fragility curves are as follows:

1. Selection of the earthquake ground motion records.
2. Normalization of PGA of the selected records to different excitation levels.
3. Making a physical model of the structure.
4. Performing a nonlinear static pushover analysis and obtaining the elastic stiffness of the structure.

5. Selection of a hysteretic model for the nonlinear dynamic response analysis.
6. Performing the nonlinear dynamic response analysis using the elastic stiffness and the selected records.
7. Obtaining the damage indices of the structure in each excitation level using a damage model.
8. Calibration of the damage indices for each damage rank to obtain the damage ratio in each excitation level.
9. Construction of the fragility curves using the obtained damage ratio and the ground motion indices for each damage rank assuming a lognormal distribution.

BRIDGE MODELS AND INPUT GROUND MOTIONS

Four typical RC bridge piers [7] and two RC bridge structures are considered of which one is a non-isolated and the other one is an isolated system. The piers are designed [8, 9] according to the 1964, 1980, 1990, and 1995 seismic design codes [10] assuming that only the size and reinforcement of the piers can be changed with other conditions such as the height of substructure (11.8m), length (35m) and weight of superstructure (23627 kN), ground condition (type II), and nominal design strength of concrete (14.7 MPa) and reinforcement (294 MPa) being unchanged. The elevation and cross-sections of the four piers are shown in Figure 1. Based on the past earthquake experience, the code requirements have been changed since 1964. One can see (Figure 1(b)) that the cross-sections and as well as the amount of both longitudinal and tie reinforcements have been changed significantly from 1964 code to 1980 code. One can also see (Figure 1(b)) that the arrangement of tie reinforcement has also been changed significantly from the 1964 code to the 1980 code. These changes have been adopted in order to have better performance of the structure against an earthquake force. However, from 1990, it can be seen that the changes are not so significant. The longitudinal reinforcement (area ratio) for the four bridge piers is taken as 1.21%, 1.25%, 1.36%, and 1.36%, respectively, while the tie reinforcement (volumetric ratio) is taken as 0.09%, 0.32%, 0.64%, and 1.03%, respectively.

In case of the two bridge models, they are designed according to the seismic design code in Japan [10] assuming that the size and reinforcement of the piers, height of the substructure, length and weight (W) of superstructure, ground condition, and nominal design strength of concrete and reinforcement being unchanged. Note that the parametric values for the two bridge systems are taken as that of the 1980 pier except for the height, which is taken as 12m. For the non-isolated bridge system, it is assumed that it has four spans with a 35m span length having 675 kN/m superstructure weight, the piers are rectangular, pin-jointed to the superstructure and fixed to the base, and the superstructure is assumed to slide on ordinary frictionless bearings at the abutments. For the isolated bridge system, a Lead-Rubber Bearing (LRB) is used as the isolation device [9, 12-16]. Kawashima and Shoji [16] recommended that the yield force of the LRB can be taken as 10-20% W, while Ghobarah and Ali [12] recommended that the yield force of the LRB can be taken as 5% W, which provides a reasonable balance between reduced forces in the piers and increased forces on abutments. However, in this study, the yield force and yield stiffness of the LRB are taken as 5% W and 5% W/mm, respectively [12]. Given the yield force level and the lead yield strength of 10-10.5 MPa [9, 12], the number and cross sectional area of the lead plugs can be designed. The advantage of LRB is that it has low yield strength and sufficiently high initial stiffness that results higher energy dissipation [9, 12-16]. The substructure stiffness for the whole bridge system is given as the sum of the stiffness of all piers [15]. The physical models of the non-isolated and isolated bridge systems are shown in Figure 2. The natural period for the non-isolated system to the longitudinal direction is 0.41s, and it shifts to 1.24s for the isolated system, which falls within the practical range of natural period for isolated systems [12, 16].

For a nonlinear dynamic response analysis and to get a wider range of the variation of input ground motion, a total of two hundred and fifty (250) records were selected from the 1995 Kobe, the

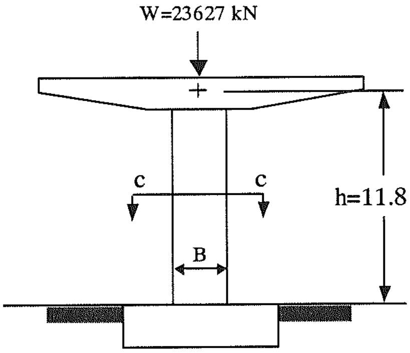

(a) Elevation of a typical bridge pier

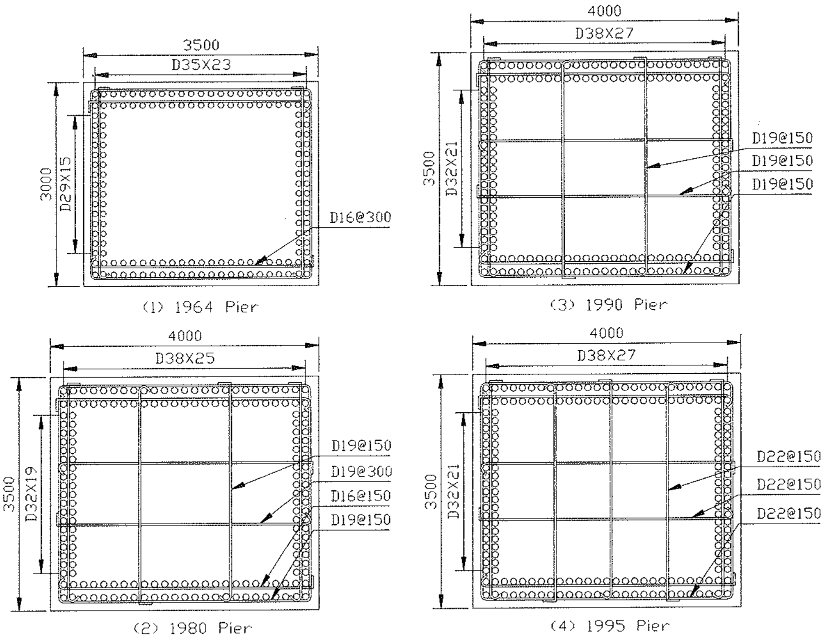

(b) Cross-sections at c-c

Figure 1. Elevation and sectional views for the four bridge piers used in this study.

1994 Northridge [17], the 1993 Kushiro-Oki, the 1987 Chibaken-Toho-Oki, and the 1999 Chi-Chi [18] earthquakes.

DAMAGE ANALYSIS AND FRAGILITY CURVES

Damage analysis

After performing the nonlinear static pushover [19, 20] and dynamic response analyses [21, 22], for the damage assessment of the structure, Park-Ang [23] damage model was used in this study. For a nonlinear dynamic response analysis, the piers and the non-isolated bridge system are modeled as a

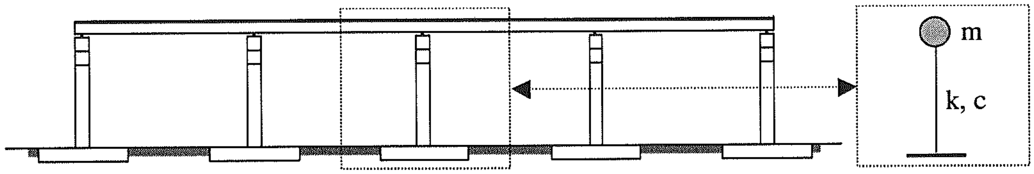

(a) Physical model of a non-isolated bridge system

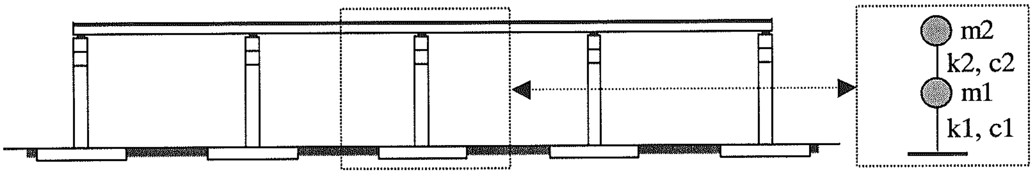

(b) Physical model of an isolated bridge system

Figure 2. Physical models of the non-isolated and isolated bridge systems used in this study.

SDOF system [9], a bilinear hysteretic model was considered [9, 22], and the post-yield stiffness was taken as 10% of the initial stiffness with 5% damping ratio [22]. For the isolated system, it is modeled as a 2DOF system [12-16], a bilinear hysteretic model was considered for the both substructure and isolation device [12, 16], the post-yield stiffness was taken as 10% of the initial stiffness for the both substructure and isolation device [9, 12, 16], the damping matrix **C** is evaluated by using the Rayleigh damping [9, 21], and the damping constant h_i is found by using the following expression [10]

$$h_i = \frac{\sum_{j=1}^{n} h_j \Phi_{ij}^T \mathbf{K}_j \Phi_{ij}}{\Phi_i^T \mathbf{K} \Phi_i} \tag{1}$$

where h_j is the equivalent damping constant of element j, Φ_{ij} is the mode vector of element j of the i-th vibration mode, $\mathbf{K}_j$ is the equivalent stiffness matrix of element j, Φ_i is the mode vector of the overall structure of the i-th vibration mode, and $\mathbf{K}$ is the equivalent stiffness matrix of the overall structure. The damage index DI is expressed as

$$DI = \frac{\mu_d + \beta \cdot \mu_h}{\mu_u} \tag{2}$$

where μ_d and μ_u are the displacement and ultimate ductility of the structure, β is the cyclic loading factor taken as 0.15, and μ_h is the cumulative hysteretic energy [24] ductility. The obtained damage indices for the selected input ground motions are then calibrated to get the damage ratio for each damage rank, which are used to construct the fragility curves [6].

Structural damage and input motion parameters

To construct a relationship between earthquake ground motion and structural damage, a data set comprising inputs (strong motion parameters) and outputs (damage) is necessary. There are two methods for doing this: 1) collect the actual earthquake records and damage data and 2) perform earthquake response analyses for given inputs and models and obtain the resultant damage (outputs). The former is more convincing because it uses actual damage data. However, earthquake records obtained near structural damage are few. With the latter, it is easier to prepare well-distributed data.

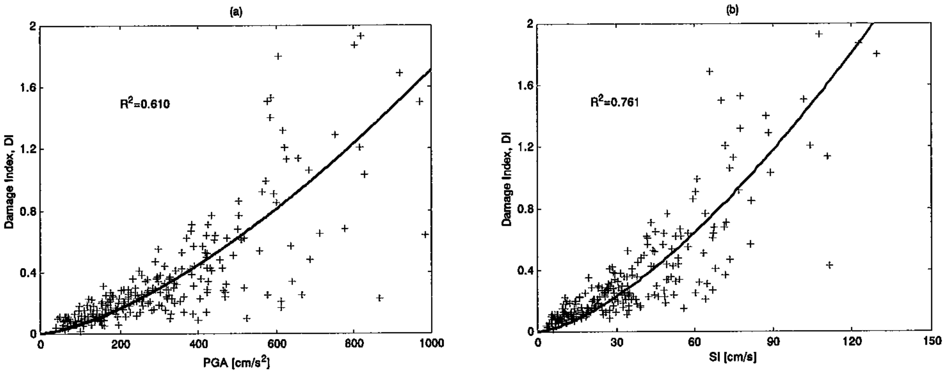

Figure 3. Relationship between (a) damage index and PGA, and (b) damage index and SI obtained from nonlinear regression analysis for the 1964 pier.

Since it is not based on actual observations, however, much care should be taken in selecting structure models and input motions. The former was used by Yamazaki *et al.* [1] and Tong and Yamazaki [25] and the latter is used in this study.

Selection of input motion parameters to correlate with the structural damage is important, however, is not an easy task. The Peak Ground Acceleration (PGA) and Peak Ground Velocity (PGV) are commonly used indices to describe the severity of the earthquake ground motion. However, it is well known that a large PGA is not always followed by severe structural damage, especially for long-period structures. Similarly, a large PGV is not always followed by severe structural damage [26], especially for the input motion including permanent fault displacements. Other indices of earthquake ground motion, e.g., Peak Ground Displacement (PGD), time duration of strong motion (T_d) [27], Spectrum Intensity (SI) [28], and spectral characteristics, can be considered in damage estimation [29].

In Japan, the JMA seismic intensity [30-32] has been used as the most important index for estimating structural damage, identifying affected areas, and preparing for crisis management due to earthquakes [33]. Also, Tokyo Gas Co. Ltd. uses the SI value [28] as the index to shut-off the natural gas supply after a damaging earthquake, and developed an SI-sensor [28] and a new SI-sensor [34, 35], which monitor both PGA and SI. Hence, it is necessary to know the correlation between the JMA seismic intensity and structural damage with other strong motion parameters. Karim and Yamazaki [36] obtained the correlation between the JMA seismic intensity with other strong motion parameters, and it was found that the JMA intensity shows the highest correlation with both PGA and SI. Similarly, the relationship between the *DI* and other strong motion parameters are obtained performing a nonlinear regression analysis [37, 38], and the regression model [25] used in this study is given as

$$y = ax^b \qquad \text{(univariate)} \qquad (3)$$

$$y = ax^b z^c \qquad \text{(multivariate)} \qquad (4)$$

where y is the *DI*, x and z are the strong motion parameters (e.g., PGA, PGV, and SI) and, a, b, c are the regression coefficients. Figure 3 shows the relationship between the *DI* and PGA and *DI* and SI obtained only from univariate regression analysis, and the coefficient of determination (R^2) are also shown in the figure. The relationship is also obtained from multivariate regression analysis, and similar to the JMA intensity, it is also found that the *DI* shows the highest correlation with both PGA and SI (R^2=0.852). Hence, fragility curves can be constructed with respect to both single and multiple ground motion parameters, however, in this study, we do restrict to consider only single ground

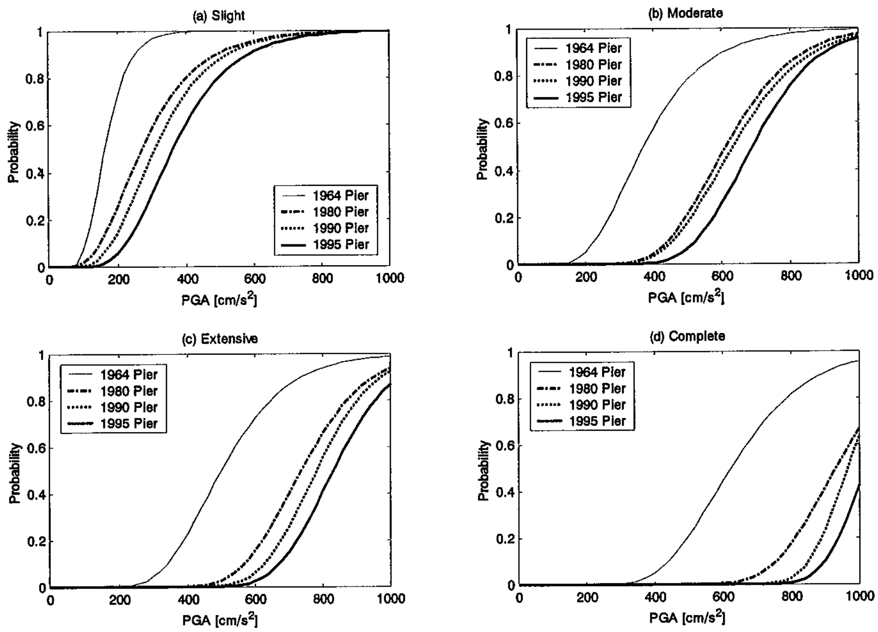

Figure 4. Comparison of the fragility curves for the four bridge piers with respect to PGA.

motion parameter, and PGA, PGV, and SI are taken as the amplitude parameters to construct the fragility curves.

Fragility curves

For the cumulative probability P_f of occurrence of the damage equal to or higher than damage rank R is given as

$$P_f(\geq R) = \Phi\left[\frac{\ln X - \lambda_x}{\xi_x}\right] \tag{5}$$

where Φ is the standard normal distribution, X is the ground motion index (e.g., PGA, PGV, and SI), λ_x and ξ_x are the mean and standard deviation of $\ln X$. Two parameters of the fragility curves, i.e., mean λ_x and standard deviation ξ_x are obtained for each damage rank by plotting the damage ratio in each excitation level on a lognormal probability paper, and performing a linear regression analysis.

Figure 4 shows the plots of the fragility curves for all damage ranks obtained for the four bridge piers with respect to PGA. One can see that the level of damage probability goes higher from 1995 pier to 1964 pier. As the code requirements changes from time to time (Figure 1(b)), the structure that is designed using the recent code is supposed to perform better against earthquake forces than the previous one does, and the evidence can be seen in the fragility curves (Figure 4). Figure 5 shows the fragility curves for the non-isolated and isolated bridge systems, and it can be seen that the level of damage probability for the isolated system is less than that of the non-isolated one. This is because the substructure experiences less lateral forces due to the energy dissipation of the isolation device. Now, it is understood that there is an effect on the fragility curves (Figures 4 and 5) due to the variation of structural parameters. It is also true that there might be an effect on the fragility curves due to the structure-soil interaction [39], however, this effect is not considered in the present study for which a

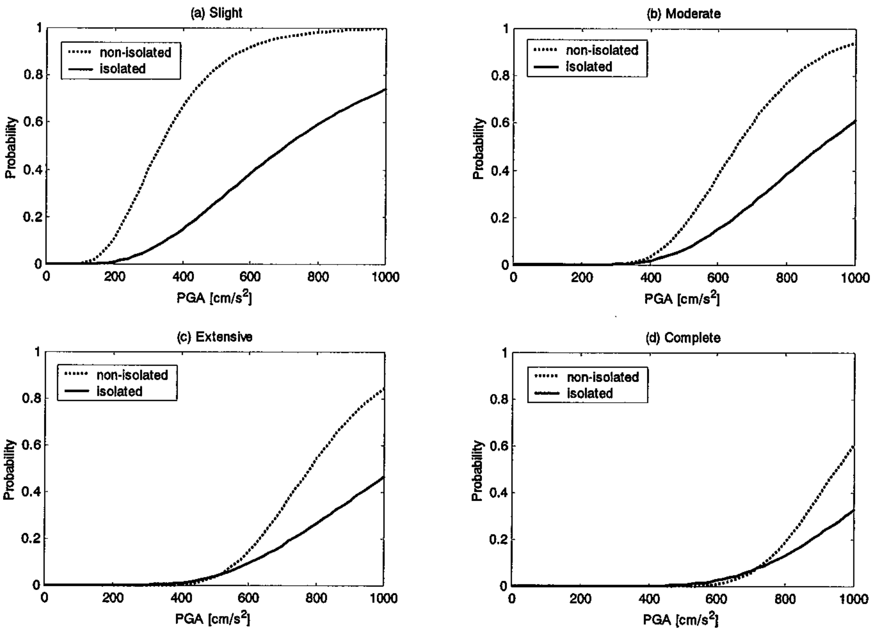

Figure 5. Comparison of the fragility curves for the non-isolated and isolated bridge systems with respect to PGA.

further research is necessary.

Relationship between the fragility curve parameters with structural parameters

It is observed (Figures 4 and 5) that if the structural parameters are changed then the fragility curves also change, in other words, there is an effect on the fragility curves due to the variation of structural parameters. However, if one looks at all these fragility curves (Figure 4) then a common trend can be seen among them. As the code requirements changes from time to time (Figure 1(b)), so, the structure that is designed using the recent seismic code has a higher strength than the previous one does, and it performs better against the seismic force than the previous one does, and the evidence can also be seen on the fragility curves (Figure 4). Hence, it is assumed that there might be a correlation between the fragility curve parameters and the structural parameters, viz., the over-strength ratio θ of the structure, height of the pier (h), span length (L), and weight (W) of the superstructure. However, for simplicity, only θ is considered in the current analysis, as it is one of the key structural parameters. The over-strength ratio θ [10] of the structure is defined as

$$\theta = \frac{P_u}{k_{he}W} \tag{6}$$

where P_u is the horizontal capacity of the structure, k_{he} is the equivalent lateral force coefficient, and W is the equivalent weight, which is calculated as the weight of the superstructure and 50% weight of the substructure [10]. The lateral force coefficient k_{he} is defined as

$$k_{he} = \frac{k_{hc}}{\sqrt{2\mu_a - 1}} \tag{7}$$

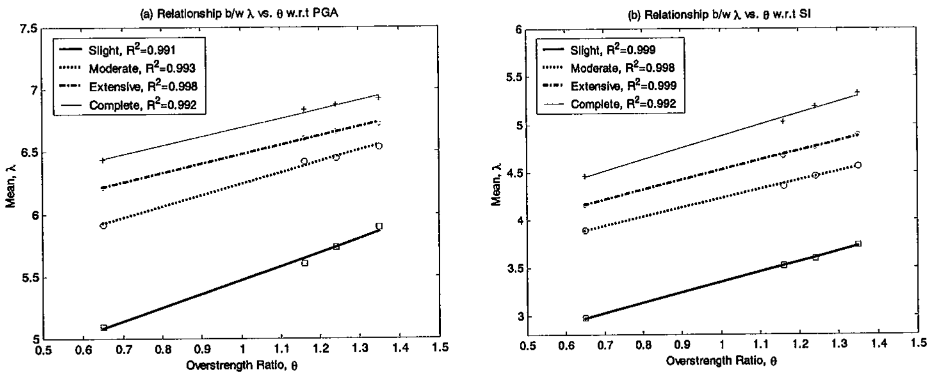

Figure 6. Relationship between fragility curve parameter λ and over-strength ratio θ of the four bridge piers used in this study (a) with respect to PGA, and (b) with respect to SI.

where k_{hc} is the design lateral force coefficient, and μ_a is the allowable ductility factor [10] of the substructure. The design lateral force coefficient k_{hc} is defined as

$$k_{hc} = c_z k_{hco} \tag{8}$$

where c_z is the zonation factor, and k_{hco} is the standard design lateral force coefficient. There are mainly three regional classes [10], viz., A, B, and C. A is defined as the region where there is higher earthquake occurrence frequency, while C is defined as the region where there is lower earthquake occurrence frequency. In this study, the region is considered as A, and the corresponding value of c_z for this region is taken as 1.0 [10]. The value of k_{hco} can be obtained knowing the fundamental period of the structure, and ground condition [10]. In this study, the ground condition is considered as type II. Note that there are two types of k_{hco}, viz., type I and II. Type I k_{hco} is defined as the design lateral force coefficient stipulated in the earlier Seismic Design Specifications (1990 code), provides seismic force that hypothesizes a large scale marine earthquake occurring on the boundary between plates. On the other hand, Type II k_{hco} is defined as the design lateral force coefficient stipulated in the recent Seismic Design Specifications (1995 code), provides seismic force that is based on acceleration strong motion records actually obtained at ground surface during the Hyogo-ken Nanbu (Kobe) Earthquake of 1995, was established by categorizing its acceleration response spectra for each ground category. In this study, k_{hco} is considered as type II. Hence, knowing the fundamental period of the structure, the standard lateral force coefficient k_{hco} can readily be obtained from the seismic design code [10].

If one looks at Equations (6) to (8), then it is obvious that the over-strength ratio θ takes into account almost all of the structural parameters, in other words, it is a function of almost all of the structural parameters. It is recommended in the code [10] that the value of θ should be greater than or equal to 1.0, however, the definition for θ is given based on the recent seismic design code [10], and the θ for the all structures are obtained based on this definition irrespective of the design codes that were used to design them. Hence, some values of θ fall below 1.0, especially, for the 1964 pier. The regression model used to obtain the relationship between fragility curve parameters λ and ξ with the over-strength ratio θ is given as

$$\lambda_\theta = b_0 + b_1\theta \tag{9}$$

$$\xi_\theta = b_0 + b_1\theta \tag{10}$$

where λ_θ and ξ_θ are the mean and standard deviation of the fragility curves with respect to θ, θ is the over-strength ratio of the structure, and b_0 and b_1 are the regression coefficients. Figure 6 shows only the relationships between the fragility curve parameter mean λ and over-strength ratio θ obtained from linear regression analysis for the four bridge piers for the all damage ranks with respect to PGA and SI, and the corresponding coefficient of determination (R^2) are also shown in the figure. Note that the data points for the isolated and non-isolated bridge systems are not included in the regression analysis as they are different systems having different pier height. It can be seen (Figure 6) that there is a very strong correlation between the fragility curve parameter λ and over-strength ratio θ, and the R^2 values are obtained for the four damage ranks with respect to PGA as 0.991, 0.993, 0.998, and 0.992, respectively, and with respect to SI, the values are obtained as 0.999, 0.998, 0.999, and 0.992, respectively. This clearly indicates that there is a strong correlation between λ and θ, and this relationship may be a very useful tool to construct the fragility curves for highway bridges knowing the θ factor only.

SIMPLIFIED METHOD TO CONSTRUCT THE FRAGILITY CURVES

Description of bridge models

In the preceding section, it is observed that there is a strong correlation between the fragility curve parameter λ with the over-strength ratio θ of the structure. However, to draw a solid conclusion, it is also necessary to consider many bridge structures that take into account all other structural parameters, for instance, span length (L), pier height (h), weight of the superstructure (W), etc. In this case, a total of thirty (30) bridge models are considered to have a wider range of the variation of structural parameters. The bridges are considered non-isolated, the piers are rectangular, pin-jointed to the superstructure and fixed to the base, and the superstructure is assumed to slide on ordinary frictionless bearings at the abutments. The ground condition is considered as type II, the regional class is considered as A, and the k_{hco} is considered as type II. The bridge models are divided in three categories, viz., bridges designed with different seismic codes, bridges having different pier heights, and bridges having different span lengths or weights, however, the number of spans for the all bridge models are assumed to be four. The substructures (piers) for any typical bridge model are considered to be similar, in other words, one pier model can be considered as the representative of all other piers for a particular bridge structure. This assumption is adopted to avoid a rigorous computation necessary to perform nonlinear pushover analysis for the all piers of a particular bridge model. The physical model is considered as the one shown in Figure 2(a), and the substructure stiffness of the whole bridge system is given as the sum of the stiffness of all piers. Table I shows all the structural properties for different categories of bridges having span length of 30m and 40m with superstructure weight as 500 kN/m. Note that same structural properties have been considered for the all bridge models having a span length of 40m, in other words, changing only the span length or weight of the superstructure while all other parameters being unchanged. It can be seen that (Table I) the pier cross section changes for different seismic design codes even having the same height, and it changes from smaller to larger from the 1964 code to the 1995 code. It can also be seen (Table I) that the pier cross section also changes due to the changes of pier height even it is designed with the same seismic code, and it changes from smaller to larger from pier height 6m to 18m. One can also see that the longitudinal (area ratio) and tie (volumetric ratio) reinforcement also changes for different seismic codes, and the value goes higher from the 1964 code to the 1995 code.

Correlation of λ and ξ with structural parameters for thirty bridge models

The fragility curve parameters λ and ξ for the thirty (30) bridge models are obtained by performing

Table I. Structural properties for the thirty (30) bridge models used in this study.

Design Code	Span Length, L=35m, 40m (w=500kN/m) — pier height (m)										reinforcement	
	6		9		12		15		18		Long.	Tie
	section		section		section		section		section		ρ_l (%)	ρ_t (%)
	a[1]	b[2]	a[1]	b[2]	a[1]	b[2]	a[1]	b[2]	a[1]	b[2]	area ratio	vol. ratio
1964	2.0	2.8	2.6	3.2	3.0	3.5	3.4	3.8	3.5	4.0	1.21	0.09
1980	2.1	3.0	2.8	3.2	3.2	3.8	3.8	4.0	3.8	4.2	1.25	0.32
1995	2.2	3.0	2.8	3.4	3.2	4.0	3.8	4.2	4.0	4.5	1.36	1.03

[1]Dimension in the longitudinal direction in m.

[2]Dimension in the transverse direction in m.

σ'_c (MPa) and σ_{sy} (MPa) are taken as the same for the all codes, and they are taken as 27 and 300, respectively.

a series of nonlinear static pushover, nonlinear dynamic response, damage, and fragility analyses using the selected two hundred and fifty (250) strong motion records. The over-strength ratio θ is calculated using Equation (6). The relationships between λ and ξ with the over-strength ratio θ only are then obtained using Equations (9) and (10) for the all damage ranks with respect to PGA, PGV, and SI considering all the data points obtained for the thirty (30) bridge models.

Figure 7(a) shows the relationship between λ and θ obtained for the slight damage with respect to PGA considering all the data points performing a linear regression analysis. It is observed (Figure 7(a)) that if all the data points are considered together without making any subgroups, for instance, data points for different codes, heights, and weights, etc., then the relationships are found not to be so good like the one as it was found (Figure 6) in case of the four bridge piers where the heights were the same. Note that the maximum R^2 for the both λ and ξ for the all damage ranks with respect to PGA, PGV, and SI is found to be 0.857. It is anticipated that fragility curve parameters might depend on other structural parameters, viz., weight of the superstructure or span length, height of the pier, and variation of the seismic codes even having the same θ value. As the bridge models are grouped mainly in three categories, hence, it is necessary to see how the weight or span length, height of the pier, and different seismic codes influence the fragility curve parameters. In order to do so, the data points are plotted for different pier heights having different superstructure weight or span length, and designed with different seismic codes.

Figure 7(b) shows the plots of λ vs. θ for different pier heights obtained from linear regression analysis, and the corresponding R^2 values are also shown in the same figure. In each level of pier height, the data points are included for different seismic codes and different superstructure weight or span length. It can be seen (Figure 7(b)) that there is a very strong correlation between λ and θ within each level of pier height like the one as it was found (Figure 6) in case of the four bridge piers where the heights were the same. Though the data points are not plotted for different weights and different seismic codes, however, as they are included within each pier height, it is clear that there is no significant effect on λ due to the variation of weights and seismic codes. This can be explained in another way: as the θ of the structure is directly related to the weight and ultimate capacity (Equation

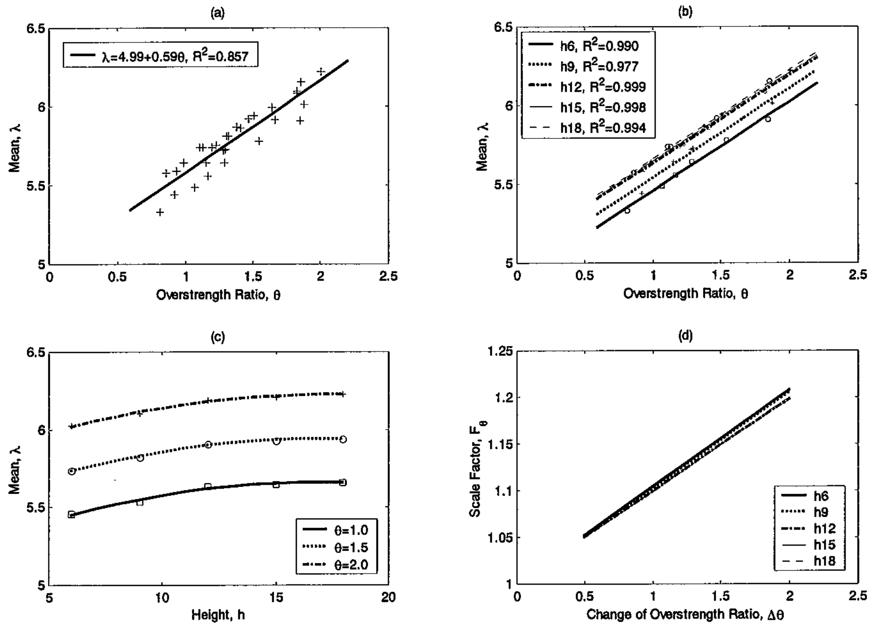

Figure 7. Relationship between (a) λ and θ obtained for the thirty bridge models used in this study, (b) λ and θ for different pier heights, (c) λ and h for different θ, and (d) F_θ and Δθ for different pier heights, all for a slight damage with respect to PGA.

(6)) of the structure, which is directly related to the seismic code used, hence, the θ takes into account the effect of both weight and the seismic design code used. It is also observed that as the code requirement changes, the θ also changes, which directly influences the λ, and the evidence can be seen in Figures 6 and 7(b), where one can see that the structure that is designed using the recent seismic code has a higher θ value, which results to have a higher λ value.

If one looks at the all relationships between λ and θ (Figure 7(b)) obtained for different pier heights, then it can be seen that the relationships are different. These relationships can be used for the bridge structure that has a pier height either any one of the heights that is considered in this study. However, practically, the pier height is rather random, and it is not possible to consider a lot of bridge models having a wide range of the variation of pier heights due to the limitations of numerical simulation, which could be solved if we could specify any stochastic model to consider the randomness of the pier heights. However, this problem has been solved in another way. First, the λ for different pier heights are obtained by fixing some θ using the relationships shown in Figure 7(b). Then the relationship between λ and h is obtained using the following regression model

$$\lambda_h = b_0 + b_1 h + b_2 h^2 \quad (11)$$

where λ_h is the mean with respect to h, h is the height of the pier, and b_0, b_1 and b_2 are the regression coefficients. Figure 7(c) shows the relationship between λ and h obtained for different θ. Like the pier height, it is also found that there is a strong correlation between λ and h for each level of θ, for instance, R^2 is found to be 0.987 for a θ value equal to 1.0. It can be seen (Figure 7(c)) that the relationships between λ and h obtained for different θ seem to be quite parallel, and it is also visible that knowing only one of the relationships between λ and h for a given θ, the other

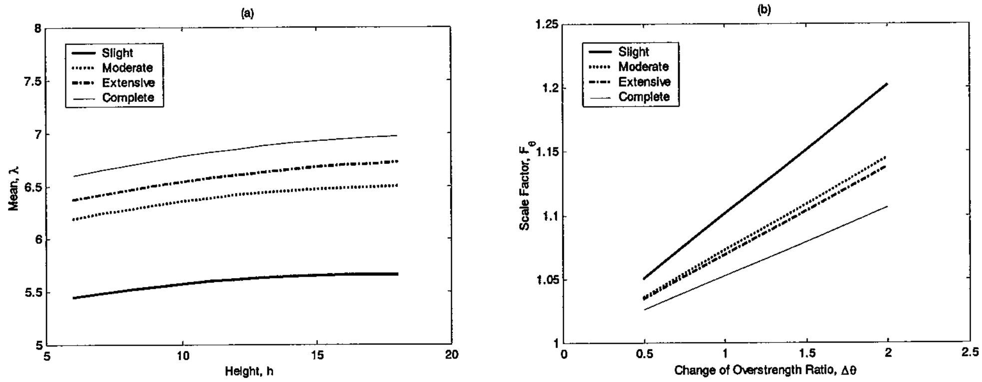

Figure 8. Relationship between (a) λ and h for θ equal to 1.0, and (b) average F_θ and Δθ obtained for different damage ranks with respect to PGA.

relationships for different θ can also be obtained knowing only some scale factors for a change of the θ. In this objective, the scale factors are obtained for changing different θ for different pier heights considering the relationship between λ and h obtained for θ equal to 1.0 as the base one, and the scale factor F_θ is given as

$$F_\theta = a_0 + a_1 \Delta\theta \quad (12)$$

where F_θ is the scale factor with respect to the change of θ, $\Delta\theta$ is the change of θ given as (θ-1), and a_0 and a_1 are the regression coefficients.

Figure 7(d) shows the relationship between F_θ and $\Delta\theta$ obtained for different pier heights, and they look very similar. However, to minimize the error that might results for different pier heights, the average scale factor obtained for different pier heights is considered in this study. Hence, the λ value can readily be obtained using Equation (11) for a known h, and then simply multiplying it by the scale factor F_θ of Equation (12) that can be obtained for a known $\Delta\theta$. In other words, the λ value can be obtained by using the following expression:

$$\lambda = \lambda_h F_\theta \quad (13)$$

Substituting for λ_h and F_θ from Equation (11) and (12) into Equation (13) gives

$$\lambda = [b_0 + b_1 h + b_2 h^2][a_0 + a_1 \Delta\theta] \quad (14)$$

From Equation (14), it can be said that λ is a function of both h and θ, and this expression might conveniently be used to obtain the λ for any given h and θ. Similar expressions are also obtained for other damage ranks, i.e., moderate, extensive, and compete. Figure 8(a) shows the relationships between λ and θ obtained for different damage ranks for θ equal to 1.0, and the corresponding average scale factors for λ obtained for different damage ranks are shown in Figure 8(b).

Similar procedure has also been adopted to obtain the expression for standard deviation ξ, and the graphical representation is shown in Figure 9 for a slight damage case. The expression for ξ is given as

$$\xi = [b_0 + b_1 h + b_2 h^2][a_0 + a_1 \Delta\theta] \quad (15)$$

Figure 10(a) shows the relationships between ξ and θ obtained for different damage ranks for θ equal to 1.0, and the corresponding average scale factors for ξ obtained for different damage ranks are shown in Figure 10(b). Equations (14) and (15) are given with respect to PGA only. Following the same procedure, the expressions for λ and ξ are also obtained with respect to PGV and SI. Finally,

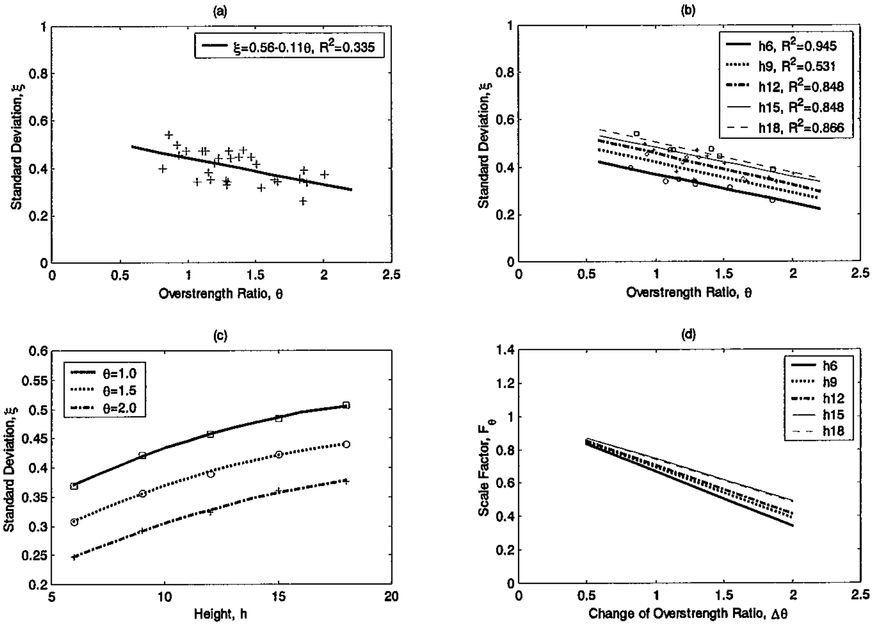

Figure 9. Relationship between (a) ξ and θ obtained for the thirty bridge models used in this study, (b) ξ and θ for different pier heights, (c) ξ and h for different θ, and (d) F_θ and Δθ for different pier heights, all for a slight damage with respect to PGA.

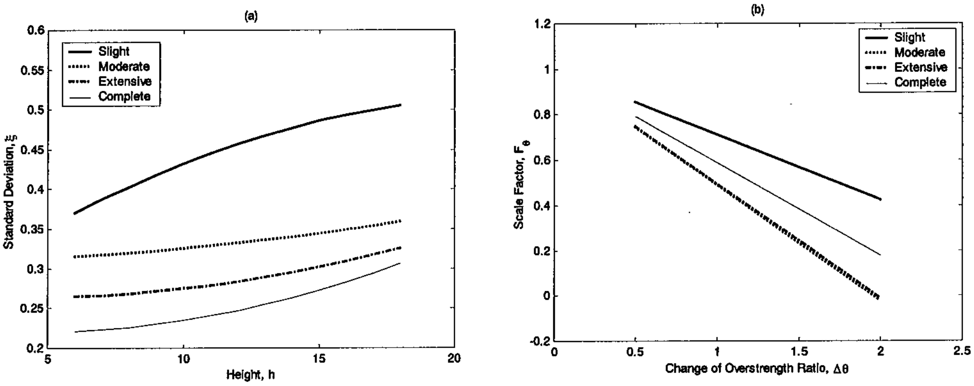

Figure 10. Relationship between (a) ξ and h for θ equal to 1.0, and (b) average F_θ and Δθ obtained for different damage ranks with respect to PGA.

the regression coefficients are obtained for the all damage ranks with respect to PGA, PGV, and SI, and the regression coefficients are shown in Table II. Note that the corresponding R^2 values are also shown in the same table. The simplified expressions (Equations (14) and (15)) obtained for the fragility curve parameters λ and ξ with respect to h and θ may be a very useful tool to construct the fragility curves of highway bridges knowing the h and θ factors only. It should be noted that the simplified expressions for the fragility curve parameters are obtained based on a set of non-isolated bridge systems, and these simplified expressions for fragility curve parameters might conveniently be

Table II. List of the regression coefficients for the fragility curve parameters obtained from the simplified method.

Indices	DR	Parameters																	
		λ									ξ								
		$\lambda_h=b_0+b_1h+b_2h^2$					$F_\theta=a_0+a_1\Delta\theta$				$\xi_h=b_0+b_1h+b_2h^2$					$F_\theta=a_0+a_1\Delta\theta$			
		b_0	b_1	b_2	σ	R^2	a_0	a_1	σ	R^2	b_0	b_1	b_2	σ	R^2	a_0	a_1	σ	R^2
PGA	S	5.16	0.06	-0.002	0.014	0.987	1.00	0.07	0.00	1.00	0.24	0.0244	-0.0006	0.002	0.999	1.00	-0.29	0.00	1.00
	M	5.82	0.07	-0.002	0.017	0.991	1.00	0.07	0.00	1.00	0.31	0.0001	0.0001	0.004	0.978	1.00	-0.51	0.00	1.00
	E	6.02	0.07	-0.002	0.021	0.989	1.00	0.05	0.00	1.00	0.27	-0.0021	0.0003	0.003	0.993	1.00	-0.50	0.00	1.00
	C	6.22	0.07	-0.002	0.005	0.999	1.00	0.06	0.00	1.00	0.23	-0.0043	0.0005	0.005	0.991	1.00	-0.41	0.00	1.00
PGV	S	2.84	0.06	-0.001	0.021	0.989	1.00	0.20	0.00	1.00	0.81	-0.0043	-0.0004	0.020	0.955	1.00	0.25	0.00	1.00
	M	3.48	0.11	-0.002	0.045	0.982	1.00	0.18	0.00	1.00	0.72	-0.0095	0.0002	0.004	0.981	1.00	0.44	0.00	1.00
	E	3.55	0.15	-0.004	0.001	0.999	1.00	0.18	0.00	1.00	0.70	0.0002	-0.0002	0.003	0.989	1.00	0.36	0.00	1.00
	C	4.32	0.08	-0.002	0.039	0.975	1.00	0.15	0.00	1.00	0.76	-0.0086	0.0002	0.004	0.981	1.00	0.34	0.00	1.00
SI	S	2.94	0.07	-0.002	0.016	0.989	1.00	0.16	0.00	1.00	0.65	-0.0185	0.0001	0.010	0.991	1.00	0.43	0.00	1.00
	M	3.60	0.09	-0.002	0.025	0.987	1.00	0.16	0.00	1.00	0.51	-0.0160	0.0002	0.006	0.994	1.00	0.99	0.00	1.00
	E	3.73	0.10	-0.003	0.009	0.999	1.00	0.16	0.00	1.00	0.43	-0.0048	-0.0003	0.012	0.974	1.00	0.84	0.00	1.00
	C	3.87	0.14	-0.004	0.031	0.985	1.00	0.19	0.00	1.00	0.33	0.0040	-0.0006	0.009	0.982	1.00	1.28	0.00	1.00

DR: Damage Rank, S: Slight, M: Moderate, E: Extensive, C: Complete.

Table III. List of the fragility curve parameters for the example bridge structure obtained from the both analytical and simplified methods.

Indices	DR	Parameters					
		λ			ξ		
		analytical	simplified	error, ε (%)	analytical	simplified	error, ε (%)
PGA	S	5.70	5.68	0.35	0.35	0.35	0.00
	M	6.46	6.39	1.08	0.24	0.26	8.33
	E	6.64	6.59	0.75	0.20	0.22	10.00
	C	6.84	6.75	1.31	0.17	0.19	11.76
PGV	S	3.47	3.46	0.28	0.82	0.81	1.21
	M	4.46	4.47	0.22	0.74	0.74	0.00
	E	4.79	4.75	0.83	0.75	0.76	1.33
	C	4.99	5.06	1.40	0.79	0.78	1.26
SI	S	3.52	3.54	0.56	0.62	0.57	8.06
	M	4.40	4.40	0.00	0.48	0.51	6.25
	E	4.65	4.56	1.93	0.46	0.47	2.17
	C	5.02	5.02	0.00	0.41	0.45	9.75

DR: Damage Rank, S: Slight, M: Moderate, E: Extensive, C: Complete.

used to construct the fragility curves of similar kind of structures. However, these expressions for the fragility curve parameters might be different for isolated bridge systems as significant difference was observed between the fragility curves of the isolated and the non-isolated bridge systems (Figure 5), and it is also anticipated that there might be an effect on the fragility curves due to the structure-soil interaction [39] for which a further research is necessary.

Numerical example

To see how the simplified expressions for the fragility curve parameters work, a different bridge structure is considered, which was not used to obtain the simplified expressions. The bridge is designed according to the recent seismic design code in Japan [10]. It is assumed that only the number of spans, span length, superstructure weight, height and cross-section of the pier can be changed while other conditions being the same as that of the thirty bridge models that were used to develop the simplified expressions. For the example bridge structure, the number of spans is assumed to be five, the length of each span is taken as 50m, the weight is taken as 320 kN/m, the height of each pier is taken as 10m, and the cross-section of each pier is taken as 2.5m by 3m. The over-strength ratio θ is calculated using Equation (6) as 1.32. Now, knowing the height of the pier as 10m and θ as 1.32, the fragility curve parameters λ and ξ for different damage ranks with respect to PGA, PGV, and SI are obtained using the simplified expressions given in Equations (14) and (15), and using the regression coefficients given in Table II. The λ and ξ are also obtained performing a series of nonlinear static pushover and dynamic response analyses.

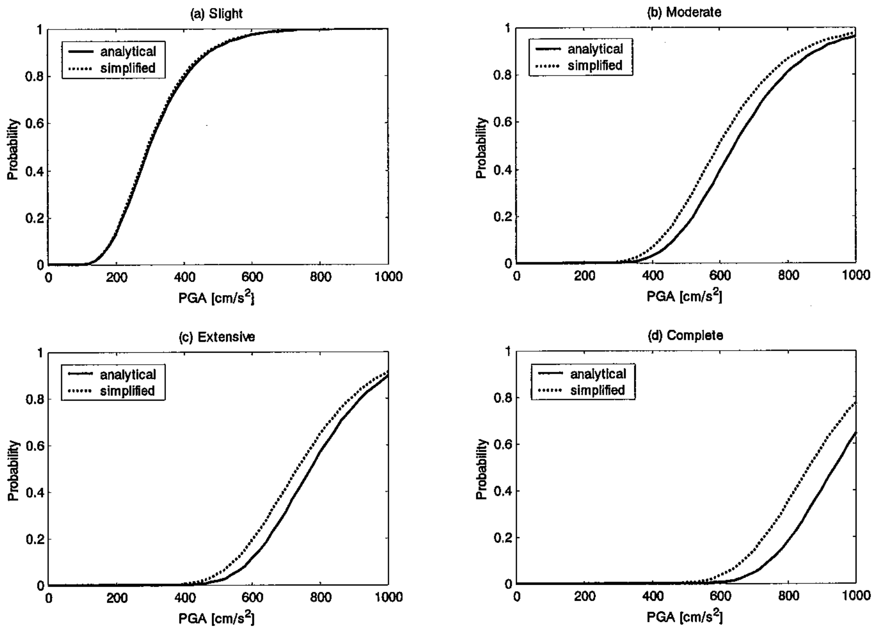

Figure 11. Comparison of the fragility curves obtained from the analytical and simplified methods for a non-isolated bridge system with respect to PGA.

Table III shows the list of the fragility curve parameters for the example bridge structure obtained from the both analytical and simplified methods, and the corresponding errors ε for the both λ and ξ with respect to the analytical one are also shown in the table. Figures 11, 12, and 13 shows the fragility curves for the all damage ranks with respect to PGA, PGV, and SI, respectively obtained from the both analytical and simplified methods. It can be seen that the fragility curves obtained by the both analytical and simplified methods seem to be very close with respect to PGV (Figure 12), and with respect to SI, they are also found to be very close except the extensive damage (Figure 13), where a small difference is found. However, with respect to PGA, a small difference is observed for the all damage ranks except the slight damage (Figure 11). Note that the maximum error with respect to PGA, PGV, and SI for the both λ and ξ are shown in Table III with an underline mark. It can be seen (Table III) that the maximum error for λ with respect to the all parameters, i.e., PGA, PGV, and SI is found to be only 1.93%, and for ξ, it is found as 11.76%. It should be noted that all the values of ξ fall below 1.0 (Table III), and the 11.76% error does not necessarily mean that it might result a significant difference between the two values, for instance, from Table III, it can be seen that the values of ξ for the analytical and simplified method corresponding to this 11.76% error are found to be 0.17 and 0.19, respectively. Hence, the error terms for the both λ and ξ given in Table III seem to be within an acceptable range, and the simplified method might conveniently be used to construct the fragility curves for non-isolated bridge structures in Japan knowing the height h and over-strength ratio θ only.

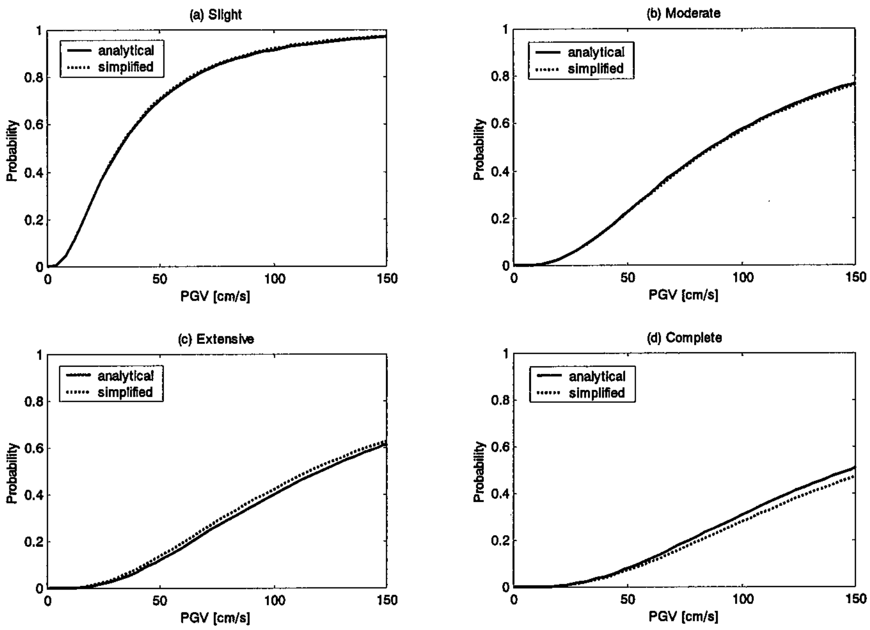

Figure 12. Comparison of the fragility curves obtained from the analytical and simplified methods for a non-isolated bridge system with respect to PGV.

CONCLUSIONS

Analytical fragility curves for the four typical bridge piers and two bridge models, of which one is a non-isolated and the other one is an isolated system, were obtained with respect to the ground motion parameters based on numerical simulation using two hundred and fifty strong motion records. Based on the nonlinear regression analysis between the damage indices of the structure with strong motion parameters, PGA, PGV, and SI were considered as the amplitude parameters for the fragility curves.

It was found that there is a significant effect on the fragility curves due to the variation of structural parameters. It was also found that the level of damage probability for the isolated bridge structure is less than that of the non-isolated one. This is because the substructure of the isolated system experiences less lateral force due to the energy dissipation of the isolation device.

It was observed that fragility curve parameters are highly correlated to the over-strength ratio of the structures. Based on this observation, a simplified method was developed to construct the fragility curves for highway bridges using thirty non-isolated bridge systems. The simplified method may be a very useful tool, and conveniently be used to construct the fragility curves for non-isolated bridge systems in Japan knowing the height of the pier and the over-strength ratio of the structure only.

It is anticipated that the simplified method developed in this study may not be applicable for the base-isolated systems as the fragility curves for the non-isolated and isolated systems were found to be rather different. It is also anticipated that there might be an effect on the fragility curves due to the structure-soil interaction. Hence, to draw a solid conclusion, it is necessary to consider these two effects for which a further research is going on.

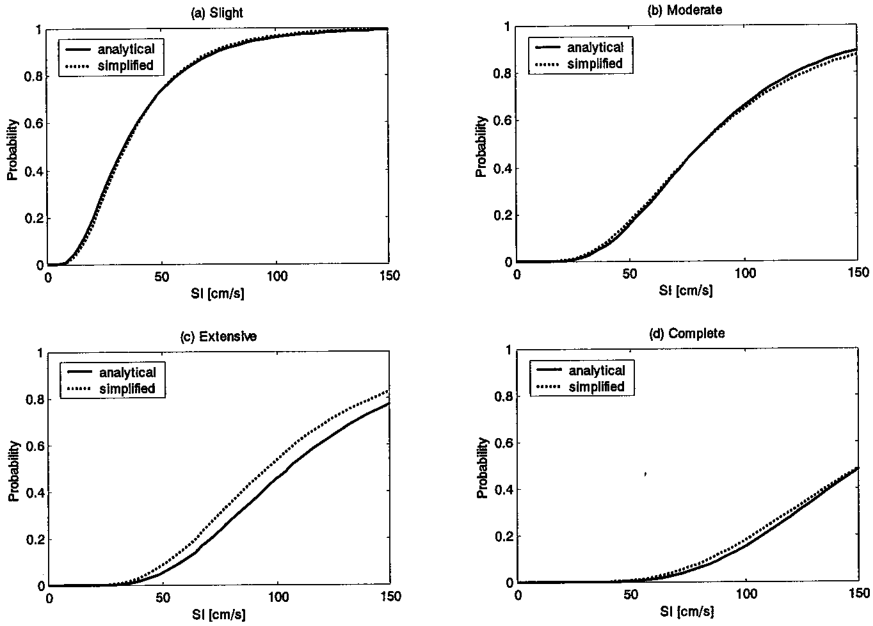

Figure 13. Comparison of the fragility curves obtained from the analytical and simplified methods for a non-isolated bridge system with respect to SI.

REFERENCES

1. Yamazaki F, Motomura H, Hamada T. Damage assessment of expressway networks in Japan based on seismic monitoring. *12th World Conference on Earthquake Engineering*, CD-ROM, 2000; Paper No. 0551.
2. Basoz N, Kiremidjian AS. Evaluation of bridge damage data from the Loma Prieta and Northridge, CA Earthquakes. *Report No. 127*, The John A. Blume Earthquake Engineering Center, Department of Civil Engineering, Stanford University, 1997.
3. Kircher CA, Nassar AA, Kustu O, Holmes WT. Development of building damage functions for earthquake loss estimation. *Earthquake Spectra* 1997; **13**(4): 663-682.
4. Ghobarah A, Aly NM, El-Attar M. Performance level criteria and evaluation. *Proceedings of the International Workshop on Seismic Design Methodologies for the next Generation of Codes*, Balkema, Rotterdam, 1997; 207-215.
5. Mander JB, Basoz N. Seismic fragility curves theory for highway bridges. *Proceedings of the 5th U.S. Conference on Lifeline Earthquake Engineering*, TCLEE No. 16, ASCE, 1999; 31-40.
6. Karim KR, Yamazaki F. Effect of earthquake ground motions on fragility curves of highway bridge piers based on numerical simulation. *Earthquake Engineering and Structural Dynamics* 2001; **30**(12):1839-1856.
7. Kawashima K, Sakai J, Takemura H. Evaluation of seismic performance of Japanese bridge piers designed with the previous codes. *Proceedings of the Second Japan-UK Workshop on Implications of Recent Earthquakes on Seismic Risk*, Technical Report TIT/EERG 98-6, 1998; 303-316.
8. Naeim F, Anderson JC. Classification and evaluation of earthquake records for design. *The 1993 NEHRP Professional Fellowship Report*, Earthquake Engineering Research Institute, 1993.
9. Priestley MJN, Seible F, Calvi GM. *Seismic Design and Retrofit of Bridges*. Wiley: New York, 1996.
10. *Design Specifications of Highway Bridges*. Part V: Seismic Design; Technical Memorandum of EED, PWRI, No. 9801, 1998.
11. Sucuoglu H, Yucemen S, Gezer A, Erberik A. Statistical evaluation of the damage potential of earthquake ground motions. *Structural Safety* 1999; **20**(4): 357-378.

12. Ghobarah A, Ali HM. Seismic performance of highway bridges. *Engineering Structures* 1988; **10**:157-166.
13. Chaudhary MTA. Evaluation of seismic performance of base-isolated bridges based on earthquake records. *PhD Dissertation*, Department of Civil Engineering, the University of Tokyo, 1999.
14. Chaudhary MTA, Abe M, Fujino Y, Yoshida J. System identification of two base-isolated bridges using seismic records. *Journal of Structural Engineering*, ASCE 2000; **126**(10):1187-1195.
15. Chaudhary MTA, Abe M, Fujino Y. Performance evaluation of base-isolated bridge using seismic records. *Engineering Structures* 2001; **23**(8):902-910.
16. Kawashima K, Shoji G. Interaction of hysteretic behavior between isolator/damper and pier in an isolated bridge. *Journal of Structural Engineering*, JSCE 1998; **44A**:213-221.
17. National Oceanic and Atmospheric Administration. *Earthquake Strong Motion CD-ROM*, National Geophysical Data Center, Boulder, 1996.
18. Central Weather Bureau. *Free-Field Strong Ground Data CD-ROM*, Seismological Center, Taiwan, 1999.
19. Bentz EC, Collins MP. Response-2000. *Software Program for Load-Deformation Response of Reinforced Concrete Section*, http://www.ecf.utoronto.ca/~ bentz/inter4/inter4.shtml, 2000.
20. SAP2000. *Integrated Structural Analysis and Design Software*, Computers & Structures Inc., 2000.
21. Chopra AK. *Dynamics of Structures: Theory and Application to Earthquake Engineering*. Prentice-Hall: Upper Saddle River, NJ, 1995.
22. Kawashima K, Macrae GA. The seismic response of bilinear oscillators using Japanese earthquake records. *Journal of Research*, PWRI, Ministry of Construction, Japan, 1993; **30**:7-146.
23. Park YJ, Ang A.H-S. Seismic damage analysis of reinforced concrete buildings. *Journal of Structural Engineering*, ASCE 1985; **111**(4):740-757.
24. Uang C-M, Bertero VV. Evaluation of seismic energy in structures. *Earthquake Engineering and Structural Dynamics* 1990; **19**:77-90.
25. Tong H, Yamazaki F. A relationship between seismic ground motion severity and house damage ratio. *Proc. of the 4th US Conference on Lifeline Earthquake Engineering*, ASCE, 1995; 33-40.
26. Loh C-H, Lee Z-K, Wu T-C, Peng S-Y. Ground motion characteristics of the Chi-Chi earthquake of 21 September 1999. *Earthquake Engineering and Structural Dynamics* 2000; **29**: 867-897.
27. Trifunac MD, Brady AG. A study of the duration of strong earthquake ground motion. *Bulletin of the Seismological Society of America* 1975; **65**:581-626.
28. Katayama T, Sato N, Saito K. SI-sensor for the identification of destructive earthquake ground motion. *Proceeding of the 9th World Con. Earthquake Engineering*, vol. 7, 1988; 667-672.
29. Molas GL, Yamazaki F. Neural networks for quick earthquake damage estimation. *Earthquake Engineering and Structural Dynamics* 1995; **24**(4):505-516.
30. Japan Meteorological Agency (JMA) *Shindo wo Shiru* (Note on the JMA seismic intensity). *Gyosei* 1996; 46-224 (in Japanese).
31. Earthquake Research Committee. Seismic activity in Japan-regional perspectives on the characteristics of destructive earthquakes-(excerpt). *http://www.hp1039.jishin.go.jp/eqchreng/eqchrfrm.htm*, 1998.
32. Shabestari KT, Yamazaki F: A proposal of instrumental seismic intensity scale compatible with MMI evaluated from three-component acceleration records. *Earthquake Spectra* 2001; **17**(4):711-723.
33. Yamazaki F, Noda S, Meguro K. Developments of early earthquake damage assessment systems in Japan. *Proc. of ICOSSAR'97*, Structural Safety and Reliability, 1998; 1573-1580.
34. Shimizu Y, Watanabe A, Koganemaru K, Nakayama W, Yamazaki F. Super high density real-time disaster mitigation system. *12th World Conference on Earthquake Engineering*, CD-ROM, 2000; 7.
35. Shimizu Y, Koganemaru K, Yamazaki F, Tamura I, Suetomi I. Seismic motion observed in Taipei basin by new SI sensors and its implication to seismic zoning. *Proc.* of the *6th Int'l Conference on Seismic Zonation*, vol. 2, 2000; 497-502.
36. Karim KR, Yamazaki F. Correlation of JMA instrumental seismic intensity with strong motion parameters. *Earthquake Engineering and Structural Dynamics* 2001 (in press).
37. Neter J, Wasserman W, Kutner MH. *Applied Linear Regression Models* (2nd edn). IRWIN: Boston, 1989.
38. Draper N, Smith H. *Applied Regression Analysis* (2nd edn). Willey: New York, 1981.
39. Chaudhary MTA, Abe M, Fujino Y. Identification of soil-structure interaction effect in base-isolated bridges from earthquake records. *Soil Dynamics and Earthquake Engineering* 2001; **21**:713-725.